Bioconjugate Chemistry

Article

pubs.acs.org/bc

# Antibody Modified Porous Silicon Microparticles for the Selective Capture of Cells

Bin Guan,[†,‡] Astrid Magenau,[‡,∥] Simone Ciampi,[†] Katharina Gaus,[‡,∥] Peter J. Reece,[⊥] and J. Justin Gooding*[,†,‡,§]

[†]School of Chemistry, [‡]The Australian Centre for NanoMedicine, [§]ARC Centre of Excellence in Convergent Bio-Nano Science and Technology, [∥]Centre for Vascular Research, and [⊥]School of Physics, The University of New South Wales, Sydney, Australia 2052

Supporting Information

**ABSTRACT:** Herein, the ability of porous silicon (PSi) particles for selectively binding to specific cells is investigated. PSi microparticles with a high reflectance band in the reflectivity profile are fabricated, and subsequently passivated and modified with antibodies via the Cu(I)-catalyzed alkyne–azide cycloaddition reaction and succimidyl activation. To demonstrate the ability of the antibody-modified PSi particles to selectively bind to one cell type over others, HeLa cells were transfected with surface epitopes fused to fluorescent proteins. The antibody-functionalized PSi particles showed good selectivity for the corresponding surface protein on HeLa cells, with no significant cross-reactivity. The results are important for the application of PSi particles in cell sensing and drug delivery.

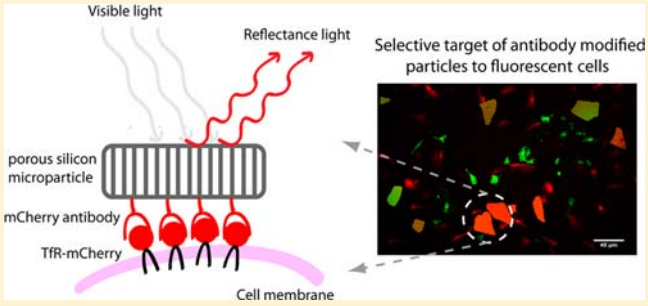


## INTRODUCTION

Nanostructured micro/nanomaterials continue to draw wide interest in diverse areas of nanotechnology and medical research. In targeted drug delivery,[1] for example, cargo-carrying nanostructured vehicles that target and attach to specific cells on diseased tissues will lead to greater drug efficacy and fewer side effects.[2,3] In the field of biosensing, especially for monitoring cell functions or cell-to-cell communication in cellular environments,[4] the potential of nanostructured sensors to provide specific targeting and attachment on single living cells is advantageous with regard to sensing sensitivity and selectivity, i.e., probing individual cells among bulk tissue.[5] To achieve this potential it is essential that the nanostructured material allows for precise control of both design and functionalization. Porous silicon (PSi) particles are a particularly attractive biomaterial for applications such as drug delivery and biosensing,[6−11] due to PSi's optical properties,[12−14] tunable nanostructures (pore size),[15−17] biocompatibility,[18−22] biodegradability,[23−25] and high capacity for therapeutics and other payloads.[25−28] Furthermore, chemical modification of PSi to stabilize the PSi structure and create various functionalities on the surfaces have been intensely investigated over the past decade.[29,30] A variety of biomolecules, such as proteins and DNAs, have been immobilized on PSi for medical and biological applications.[31−35] The in vivo uses of PSi particles as therapeutic and diagnostic agents have also been demonstrated.[36−38]

Surface properties of the nanostructured materials play an important role in cell–material interactions.[39] To gain a firm control over the specificity of the interaction and prevent possible interference from other molecules in the cellular environment, it is critical to fabricate a suitable interface to target and attach individual cells. Antibodies are considered ideal biorecognition elements due to the specificity and high affinity they can have for their cognate antigen.[40−44] For example, DeLouise et al. have demonstrated the applications of PSi for detecting protein or drugs based on affinity binding between antibody and antigen.[45,46] Recently, a group of antibody-functionalized PSi nanoparticles loaded with anticancer drugs were reported to successfully target cancer cells, such as neuroblastoma, glioblastoma, and B lymphoma cells.[35] However, no information on the selectivity of the target was provided.

To explore the potential of PSi particles in targeting specific cellular subtypes, we investigated the ability of PSi particles to selectively bind to individual cells for future drug delivery or sensing applications. PSi microparticles with unique reflectivity profiles were passivated and functionalized with antibodies on their surfaces, being able to target and capture cells presenting a specific surface epitope via the antibody–epitope affinity. An established tissue culture strain of human epidermoid carcinoma cells, HeLa cells, was employed in this study as a model cell line. Cells were transfected to express proteins with extracellular epitopes on the membrane. We chose to express fluorescent proteins with glycophosphatidylinositol (GPI) motifs or the human transferrin receptor (TfR) as the

**Received:** April 1, 2014
**Revised:** May 26, 2014
**Published:** June 3, 2014





dx.doi.org/10.1021/bc500144u | *Bioconjugate Chem.* 2014, 25, 1282−1289

**Scheme 1. Stepwise Surface Modification of Freshly Prepared PSi Lift-Off Films**[a]

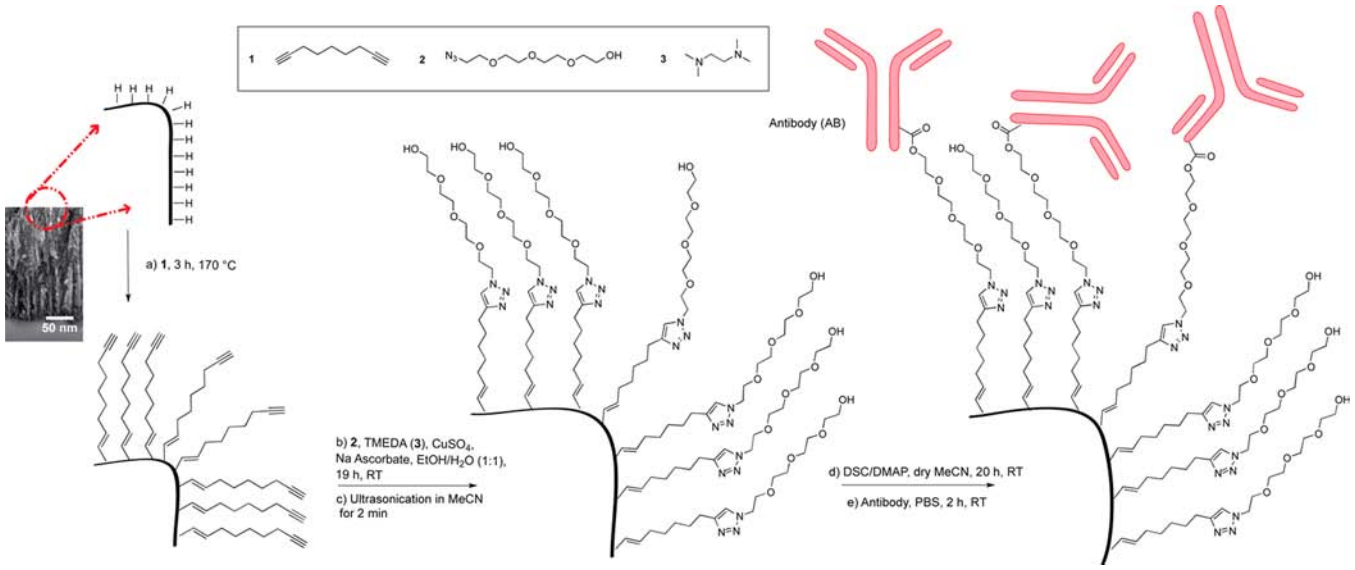


[a](a) Hydride-terminated surface was hydrosilylated with dialkyne species **1** to afford a passivated surface. (b) CuAAC "click" reaction with azide compound **2** in the presence of $Cu^{I}$ stablizing ligand **3** was performed to decorate the surface with antifouling tetra(ethylene glycol) ($EO_4$) moieties. (c) The derivatized PSi free-standing film was fractured into particles via ultrasonication. (d, e) The $EO_4$ terminated PSi particles were further functionalized with antibodies via succinimidyl activation, yielding antibody-modified PSi particles.

membrane anchor, which results in the localization of green fluorescence protein (GFP) or mCherry in the outer leaflet of the plasma membrane. Hence it was relatively simple to identify whether the correct particles have bound to the correct GPI-GFP or TfR-mCherry expressing cells by matching their respective colors. Thus, the specificity and selectivity of the interaction was demonstrated for antibody-modified PSi particles and transfected HeLa cells.

## RESULTS AND DISCUSSION

**Antibody Functionalized PSi Particles.** We fabricated PSi microparticles as outlined in Scheme 1. Briefly, a free-standing film of freshly prepared hydride-terminated PSi was passivated with dialkyne, 1,8-nonadiyne in an inert atmosphere at 170 °C for 3 h, yielding a surface with an alkyne distal terminus. Subsequently, ethylene glycol "antifouling" moieties were grafted onto the distal alkyne in the presence of a Cu(I) catalyst via the Huisgen 1,3-dipolar cycloaddition reaction (CuAAC, "click" reaction). The resulting antifouling PSi film was then fractured by an ultrasonic tip in acetonitrile to yield micrometer-sized PSi particles (mostly 20 to 80 $\mu$m in Feret diameter, Supporting Information Figure S1) with the surface functional groups unaltered.[47] The ethylene glycol moieties on the surfaces of particles were easily activated via a succinimidyl linker, disuccinimidyl carbonate (DSC), and reacted with the primary amine groups from the amino acids of the antibodies. Hence, antibodies were covalently attached onto the functionalized PSi particles.

Each step of surface modification was characterized by transmittance Fourier transfer infrared spectroscopy (FTIR), as shown in Figure 1. The presence of $\nu(C{\equiv}CH)$, $\nu_a(CH_2)$, $\nu_s(CH_2)$, $\nu(SiC{=}C)$, and $\delta(CH_2)$ modes in Figure 1a at 3310, 2930, 2850, 1595, and 1440 $cm^{-1}$, respectively, suggests the formation of an alkenyl (Si−C═C−R) acetylene-terminated monolayer on PSi surface.[48] After CuAAC "click" reaction, a significant decrease of the $\nu(C{\equiv}CH)$ mode at 3310 $cm^{-1}$ and the appearance of $\nu(C{-}O{-}C)$ mode at 1150 $cm^{-1}$ and broad

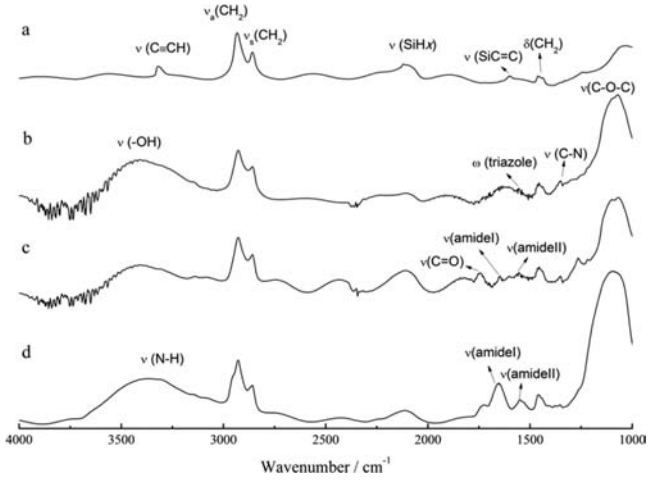


**Figure 1.** Transmission-mode FTIR spectra of (a) acetylenyl terminated PSi film, (b) tetra(ethylene glycol) moieties modified PSi particles, (c) particles after DSC activation, and (d) antibody coupling.

hydroxyl vibration (−OH) at 3500−3200 $cm^{-1}$ from ethylene glycol moiety were observed (Figure 1b), complying with $EO_4$ derivatization on the surface of PSi particles. Moreover, the weak IR peaks at 1550 and 1350 $cm^{-1}$ (Figure 1b), are ascribed to the stretching of triazole ring and C−N bonding,[49,50] providing further support for the success of the "click" reaction and the formation of $EO_4$ terminated particles. In Figure 1c, the appearance of IR stretching at 1750 and 1650 $cm^{-1}$, attributed by C═O from the carbonate group and amide I from the succinidimyl groups respectively, and the slight attenuation in $\nu(-OH)$ stretching suggest successful activation of the distal hydroxyl group of ethylene glycol to a succinimide ester. The amide II mode was weak and overlapped with a stretch from the triazole ring at 1550 $cm^{-1}$. After incubating the activated particles in antibody solution, the intensity of the C═O stretching decreases as shown in Figure 1d. Instead, the


dx.doi.org/10.1021/bc500144u | Bioconjugate Chem. 2014, 25, 1282−1289

increase of two peaks at 1650 and 1550 $cm^{-1}$, ascribed to amide I and amide II from peptide bonds,[51] confirm the successful coupling of antibody on PSi particles. The increase of the broad peak at around 3400 $cm^{-1}$, corresponding to −OH or N−H stretching from the amino acids of antibodies also indicates the antibody-coupled surface on PSi particles.

The antibody-modified particles were further examined for the ability to interact with corresponding biomolecules. For example, antibovine serum albumin (BSA) antibodies modified PSi particles demonstrated higher affinities to free FITC-labeled BSA in solution, compared to non-antibody modified particles. The detailed results, which are presented in Supporting Information Figure S2, verify again the well-developed antibody functionalization on PSi particles.

**Cell-Targeting with Functionalized Particles via Antibody−Antigen Binding.** The binding of antibody-modified particles to cells presenting antibody epitopes was then examined. HeLa cells were transfected with glycosylphosphatidylinositol (GPI)-GFP plasmid DNA, which causes the HeLa cells to express green fluorescent protein (GFP) on the cell membrane. Anti-GFP antibody, which specifically binds to GFP presenting on the cell membrane, was immobilized onto PSi particles. Anti-GFP particles and GPI-GFP-transfected HeLa cells were then incubated together to be examined for the interaction between surface-bound antibody and cell-expressing receptor protein. In order to investigate the specificity of this binding, several control experiments were performed in parallel. Since transferrin receptor (TfR) is ubiquitously expressed on HeLa cells, PSi particles modified with anti-TfR antibodies acted as a positive control. Anti-BSA derivatized particles were used as a negative control, as anti-BSA antibodies do not have any affinity for GFP on cell membranes. $EO_4$-terminated antifouling particles were also employed to exclude the possibility of nonspecific binding.

Fluorescence microscopy was utilized to examine the interaction between PSi particles and HeLa cells. The images of PSi particles were recorded under bright-field transmission mode, while HeLa cells expressing fluorescent proteins were observed in epifluorescence mode with suitable emission filters. Each image covers an area of 340 $\mu$m × 256 $\mu$m. The micrographs and statistical analysis are displayed in Figure 2. Figure 2a shows anti-GFP particles adhering closely to the well-spread transfected HeLa cells that display green fluorescence in Figure 2b. This figure demonstrates successful targeting of anti-GFP particles to GFP-transfected cells. Note that not all HeLa cells are transfected and hence do not emit a GFP signal. Transfected HeLa cells exhibit varying levels of fluorescent intensity due to the variation in the extent of GPI-GFP expression.[52] Figure 2c,d shows similar images for anti-GFP and anti-TfR particles adhering onto HeLa cells. Subsequently the number of antibody modified particles per image region (being the bottom of the cell culture plate with a diameter of 15.6 mm) on fluorescent HeLa cells was calculated for statistical analysis.

In parallel, the interaction of transfected HeLa cells with anti-TfR, anti-BSA modified particles, and with particles rendered antifouling by modifying with $EO_4$, was conducted. Antifouling/anti-BSA particles associated with transfected cells were illustrated in Supporting Information Figure S4. The results for different antibody-coated particles were displayed and compared as shown in Figure 2e. One-way ANOVA analysis[53] was performed to show that there was a significant difference between the numbers of anti-GFP/anti-TfR particles and anti-

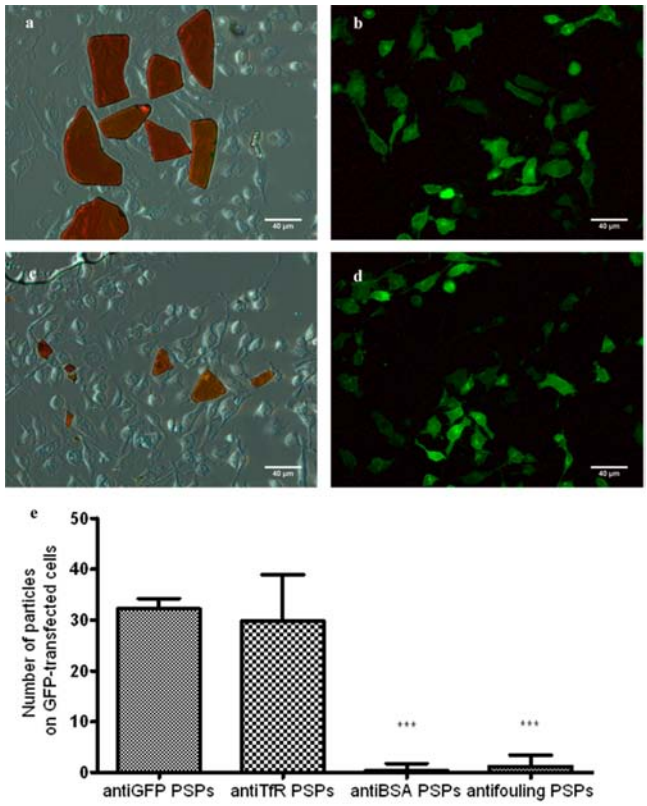


**Figure 2.** (a,b) Bright-field microscopy image (a) and fluorescence image (b) of anti-GFP-coated porous silicon particles (PSPs) bound to GPI-GFP transfected HeLa cells. (c,d) Bright-field micrograph (c) and fluorescence image (d) of anti-TfR PSPs and GPI-GFP-transfected HeLa cells. (e) Number of antibody-modified PSPs that were attached to GFP-transfected HeLa cells (anti-GFP PSPs) and HeLa cells (anti-TfR PSPs, anti-BSA PSPs, antifouling PSPs). A total of 40 particles per condition were examined. Asterisks represent significant differences to the number of anti-GFP modified particles, based on one-way ANOVA analysis (*** $P < 0.01$). Scale bars are 40 $\mu$m.

BSA/antifouling particles bound to GPI-GFP transfected cells. Both anti-GFP and anti-TfR particles were found to bind to transfected cells, as both antibodies had bound to epitopes on the cell membrane. Only a few anti-BSA and antifouling control particles bound to transfected cells, which confirmed that the binding of anti-GFP particles and GPI-GFP transfected cells was reasonably specific. Hence, these antibody-modified PSi particles can be further used to capture specific types of cells for therapeutic applications. Note that due to the uneven distribution of particle size after sonication (mostly from 20 to 80 $\mu$m, see Supporting Information Figure S1c), there are some particles that captured more than one transfected cells. However, the diversity in PSi particle size had no direct influence on the specificity of the cell−particle interaction. A more homogeneous particle size could be achieved by selecting specific sizes with a sieve or filter,[54] and hence the specific targeting of one single cell with one particle could be realized.

**Selective Capture of Different Types of Cells with Functionalized PSi Particles.** Considering the complexity of the biological system, it is also important to test the binding selectivity of antibody-modified PSi particles to cells presenting antibody receptors for the development of drug carriers or cell sensors based on PSi particles. Two pairs of cells and modified particles were employed to demonstrate the selective

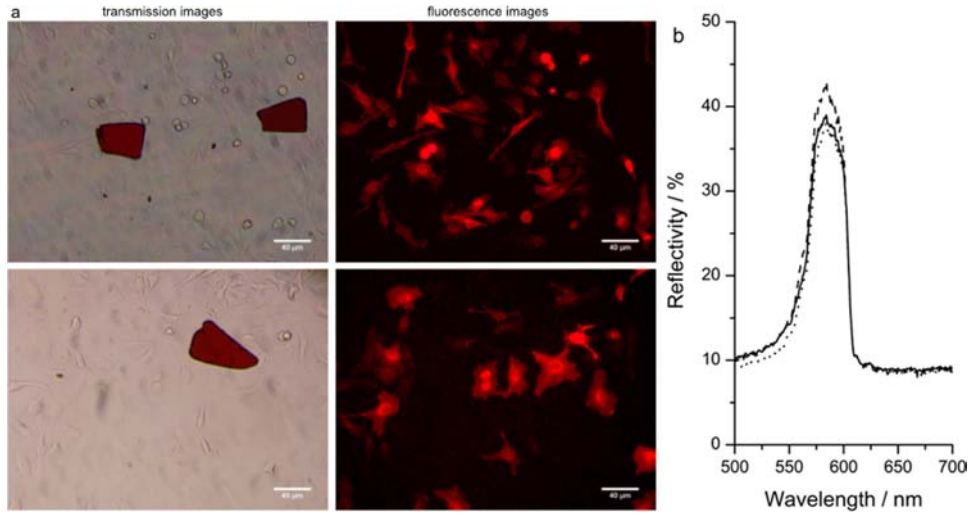


**Figure 3.** (a) Brightfield images (left side) and fluorescence images (right side) of anti-mCherry modified particles and TfR-mCherry transfected HeLa cells. The cells were first imaged in brightfield and fluorescence mode before measuring the reflectivity of the same image region. (b) Reflectivity spectra of anti-mCherry modified particles showing a reflectance band at about 590 nm.

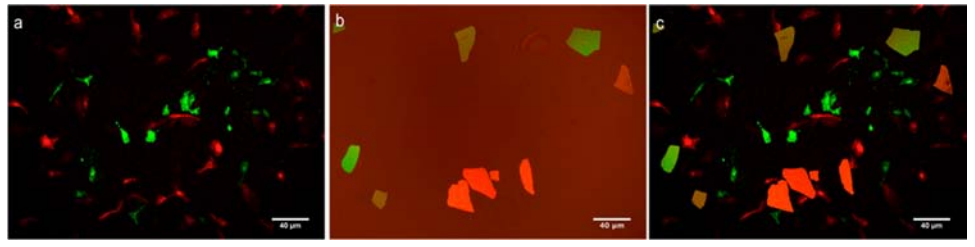


**Figure 4.** (a) Merged fluorescence images of GPI-GFP (green) and TfR-mCherry (red) transfected cells, (b) corresponding reflectance image of green and red PSi particles with anti-GFP and anti-mCherry functionalization, respectively, and (c) overlay image showing the differently functionalized PSi particles attached to their cells. Scale bars are 40 $\mu$m.

interaction between cells and particles in a cocktail of more than one cell type. Anti-GFP modified particles and GPI-GFP transfected HeLa cells, as described in the previous section, have high selectivity and affinity to each other. Similarly, anti-mCherry-modified particles and TfR-mCherry transfected cells were chosen as the second pair of cell type and matched sensor.

The binding affinity of the anti-mCherry-derivatized particles to TfR-mCherry transfected HeLa cells was investigated first. Similar to the GPI-GFP marker, anti-mCherry particles and mCherry-presenting cells were thoroughly mixed and incubated together. After washing to remove nonadhered particles, the interaction between anti-mCherry particles and TfR-mCherry-transfected cells was examined under on a microscope in bright-field and epifluorescence mode, respectively. Figure 3a displays the micrographs of anti-mCherry particles and the red fluorescent, transfected mCherry-expressing cells. The left panel exhibits shows particles and cells under brightfield illumination, while the right panel shows the fluorescence of the transfected cells. From these images, it can be concluded that the anti-mCherry particles were attached to the red fluorescent cells (TfR-mCherry transfected cells), confirming a high affinity of antibody-coated particles to transfected cells.

The PSi particles can be engineered to reflect different wavelengths of light such that they look different colours. The reflectivity spectra of anti-mCherry particles, that were adhered to cells, were recorded on the same microscope with a custom-built optical setup. As shown in Figure 3b, the reflectivity peak of anti-mCherry particles was at 590 nm, which means that the particles exhibit a red color under the reflectance imaging mode. In order to distinguish the particles functionalized with anti-GFP antibodies from those with anti-mCherry antibodies in the following experiment, anti-GFP particles were engineered with the central wavelength of 550 nm, i.e., showing in green in reflectance mode (Supporting Information Figure S3).

The two matched pairs of transfected cells and antibody-coated particles were mixed and incubated. Prior to imaging, cells were carefully rinsed to remove any nonadhered particles. The images of antibody-coupled particles and transfected cells were captured in three different imaging modes: brightfield transmission, reflectance mode, and epifluorescence (with filters for green and red emission bands, respectively). The binding selectivity of antibody-modified PSi particles to cells was determined by examining the number of particles attached to the corresponding cells. This was quantified by overlaying transmission and epifluorescence images and counting the number of particles bound to the respective cell type.

Figure 4 shows the overlay of fluorescence images of GPI-GFP and TfR-mCherry transfected HeLa cells with images of anti-GFP PSi particles in green and anti-mCherry particles in red acquired in reflectance mode. The images show that the red anti-mCherry particles were predominately bound to red fluorescent TfR-mCherry transfected cells and green anti-GFP particles were mainly found on or near green GPI-GFP transfected cells.


dx.doi.org/10.1021/bc500144u | *Bioconjugate Chem.* 2014, 25, 1282−1289

The number of antibody-coated particles bound to the corresponding transfected cells and nontransfected, nonfluorescent cells was counted and compared in Figure 5. The

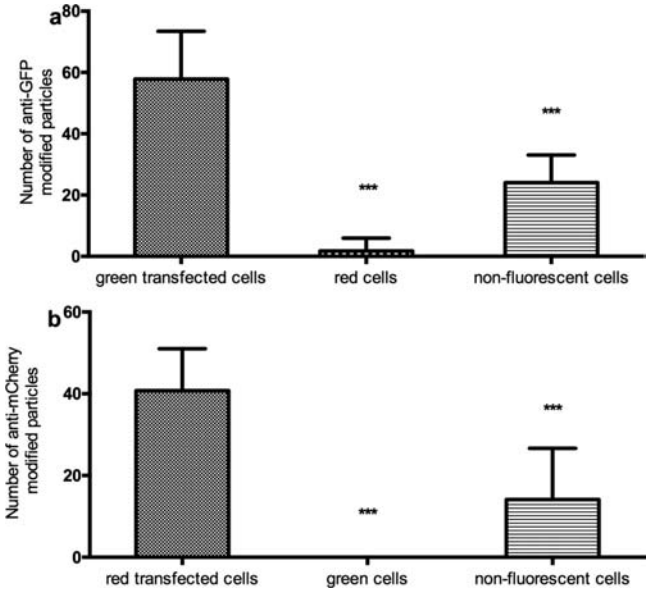


**Figure 5.** Statistic analysis of the selective capture of specific fluorescent protein-presenting cells by antibody-modified particles. (a) Number of anti-GFP particles binding to green GPI-GFP expressing HeLa cells, red TfR-mCherry expressing HeLa cells, and nonfluorescent HeLa cells. (b) Number of anti-mCherry particles on the three different types of cells. A total of 100 anti-GFP and anti-mCherry particles were examined. Asterisks represent significant differences relative to particle number on GPI-GFP-positive cells, based on one-way ANOVA analysis (***$P < 0.0001$).

statistical analysis of the number of anti-GFP and anti-mCherry particles, which were attached to either transfected cells or nontransfected cells, was performed based on the results from seven repeats of the experiment. The performance of anti-GFP particles capturing GPI-GFP-presenting HeLa cells from the cell mixture is summarized in Figure 5a. There are three scenarios for cell−particle interaction: anti-GFP particles binding to GPI-GFP-transfected expressing cells as expected, anti-GFP particles binding to TfR-mCherry-transfected expressing cells and to cells that were exposed to the tranfection reagents but did not exhibit strong fluorescence. One-way ANOVA analysis reveals a significantly larger number of anti-GFP particles adhering onto GPI-GFP expressing cells than to non-GFP expressing or TfR-mCherry expressing cells, suggesting selective binding between anti-GFP particles and GPI-GFP expressing cells. Note that in Figure 5a, there are some anti-GFP particles targeting cells that did not express detectable levels of GFP. During transfection, the amount of plasmid DNA entering into the cell nuclei and the extent of protein expression differs for each individual cell. As a consequence, the concentration of GPI-GFP or TfR-mCherry molecules on the membrane of each transfected cell varies. Hence, some seemingly nontransfected cells, i.e., nonfluorescent cells may also possess a small amount of GPI-GFP or TfR-mCherry molecules so that the binding to apparent nonfluorescent cells is higher than to TfR-mCherry and GPI-GFP-expressing cells respectively, which are truly negative of the epitope recognized by the modified particles.

In the case of anti-mCherry particles and transfected cells as shown in Figure 5b, there is a significantly greater number of anti-mCherry particles targeting TfR-mCherry expressing cells, compared to the same type of particles adhering to GPI-GFP expressing cells or nonfluorescent cells. With most of the anti-mCherry particles attaching to the corresponding mCherry-positive cells, the data again suggest the selectivity of cell−particle interaction. No anti-mCherry particles were observed on GFP-transfected cells, illustrating the lack of nonspecific binding of anti-mCherry particles to other transfected cells. There were some antibody-coated particles found on non-transfected fluorescence cells, that may be attributed to the diversity of expression of the epitope of fluorescent protein across the cell population. Accordingly, it can be concluded that both anti-GFP and anti-mCherry PSi particles were able to selectively capture GPI-GFP and TfR-mCherry expressing cells, respectively, without leading to significant nonspecific binding.

## CONCLUSION

PSi microparticles are attractive for a variety of bioapplications due to the tunable porous structure, the optical properties, and the biocompatibility. Particularly, PSi with a metastable silicon-hydride surface can be chemically functionalized, giving rise to various funtionalities on the surface, such as the antibody-derivatized PSi surface presented in this paper. The antibody-functionalized PSi particles were demonstrated to specifically and selectively target and capture cells presenting receptors or fluorescent proteins via antibody−antigen binding. These PSi particles, targeting corresponding cells, retained their optical reflectivity signals, and were able to conduct label-free biosensing or in situ monitoring of drug payload in the process of loading and releasing to targeted tissues. More importantly, by controlling the particle size during sonication,[55] the functionalized PSi particles should be able to capture single cells. This potential provides a tool for single-cell study to undestand the mechanism and function of each cell in detail, which is vital for drug discovery, toxicology studies, and other cell biology research.[56−59]

## EXPERIMENTAL PROCEDURES

**Fabrication of PSi Microparticles.** Formation of PSi microparticles followed the same engineering steps as described previously.[47] In brief, (100)-oriented p-type single-crystal Si wafers (0.06−0.07 ohm.cm, Siltronix) were electrochemically etched by a variable current density in the range of 42 mA·cm$^{-2}$ and 124 mA·cm$^{-2}$ to form rugate filter structures in an electrolyte containing aqueous 48% hydrofluoric acid and ethanol absolute in a 1:1 (v/v) ratio. The resulting PSi films with 60 periods of low and high refractive index layers were lifted from the substrate by a high current pulse (11.3 mA·mm$^{-2}$) in a solution of 15% hydrofluoric acid (v/v) in ethanol.

The freshly etched free-standing PSi films were modified with 1,8-nonadiyne (Alfa Aesar, 97%, redestilled from sodium borohydride under reduced pressure and stored under the protection of dry argon) in a dry argon atomsphere at 170 °C for 3 h to form acetylene monolayers on the surface. Cu$^{I}$-catalyzed alkyne azide cycloaddition (CuAAC) "click" reaction was performed on the acetylene-terminated samples with 11-azido-3,6,9-trioxaundecan-1-ol overnight in the presence of Cu$^{I}$-stabilizing ligand, *N,N,N′,N′*-tetramethylethane-1,2-diamine, yielding tetra(ethylene glycol) ($EO_4$) terminated PSi films. Then, the functionalized lift-off samples were shattered

into microparticles in acetonitrile via microtip ultrasonication. The particles were vacuum-dried and stored under argon for further use.

**Immobilization of Antibodies onto Functionalized PSi Particles.** The PSi microparticles with distal $EO_4$ motifs were first activated with disuccinimidyl carbonate (DSC) in dry acetonitrile to form succinimidyl ester groups on the surface. The activated particles were incubated with primary green fluorescence protein (GFP) antibody solution (20 $\mu$g/mL, Abcam) in phosphate buffered saline (PBS), and red fluorescent protein mCherry monoclonal antibody solution (2 $\mu$g/mL, Clontech), respectively, for 2 h at room temperature, affording antibody-coupled surfaces. The anti-GFP and anti-mCherry modified particles were then rinsed twice with PBS washing buffer (containing 0.5% (v/v) Tween 20, Sigma-Aldrich), followed by copious rinsing of PBS and stored at 4 °C. In the same way, ah (aryl hydrocarbon) receptor anti-transferrin (TfR) IgG (Santa Cruz) and anti-bovine serum albumin (BSA) antibodies (Sigma-Aldrich) were immobilized onto PSi particles for further experiments.

**Cell Culture and Transfection.** HeLa cells were cultured in Dulbecco's Modified Eagle Medium (DMEM, Invitrogen) with 10% fetal bovine serum (FBS) and L-glutamine at 37 °C at 5% $CO_2$ until confluency (around $1\times 10^6$ cells per mL). Cells were harvested with a 0.25% trypsin solution in PBS, suspended in full DMEM with 10% FBS, and L-glutamine and replated in a 24-well plate at density of $1.5\times 10^5$ to $2\times 10^5$ per well. The transfection mixture consisted of 0.5 $\mu$L of GPI-GFP transfecting plasmid DNA or TfRGPI-mCherry transfecting DNA, 1 $\mu$L Lipofectamine LTX Reagent (Invitrogen), and 50 $\mu$L Opti-MEM reduced serum media. Prior to addition to the cells, the mixture was incubated at 37 °C for at least 15 min before 51.5 $\mu$L of the transfection mixture was added to each well of a 24-well plate. The cells were then incubated for 18 to 30 h at 37 °C in 5% $CO_2$.

**Interaction between the Transfected HeLa Cells and Functionalized PSi Particles.** Transfected HeLa cells in the 24-well plate were harvested with a 0.25% trypsin solution in PBS, suspended in full DMEM with 10% FBS and L-glutamine. The cell suspension was then transferred into a sterile centrifuge tube and centrifuged at 1500 rpm for 5 min. The supernatant was discarded and cells were resuspended in 1 mL full DMEM. Anti-GFP, anti-TfR, and anti-BSA antibody-modified PSi particles, as well as antifouling $EO_4$ particles, were respectively added to the cell suspension. Each centrifuge tube with one type of functionalized particles and transfected cells was incubated at 37 °C in 5% $CO_2$ for 30 min, while being shaken gently every 10 min to mix particles and cells. Finally, the mixture of particles and cells was replated into a well of 24-well plate and incubated at 37 °C in 5% $CO_2$ for 4 h. Adhered cells and particles in the wells were then washed twice with PBS and fixed in with 4% (v/v) paraformaldehyde (PFA) in PBS at room temperature in the dark for 15 min, followed by rinsing twice with PBS. Cells and particles were either imaged immediately, or stored in the dark at 4 °C.

For investigating the selective binding of antibody-modified particles to receptor-presenting HeLa cells, the following experiment was performed. GPI-GFP and TfR-mCherry transfected HeLa cell suspensions were prepared as described above and then mixed together. Anti-GFP and anti-mCherry particles were added to the cell suspension. After mixing, replating, and incubating for 4 h, cells and particles in the well were washed twice with PBS, fixed with 4% (v/v) PFA in PBS, and imaged.

**Characterization and Data Analysis.** The Spotlight 400 Fourier transfer infrared spectroscopy (FTIR) Microscope system (PerkinElmer) was used to record transmission FTIR spectra from PSi free-standing films and single PSi particles. The films or particles were vacuum-dried and mounted on a potassium chloride disc. The spectra were then collected at the resolution of 2 $cm^{-1}$ and an average of 128 scans with the light aperture of $45\times 45$ $\mu m^2$.

Optical reflectivity spectra of the microparticles were measured in a custom built optical setup on an inverted Leica DM IL LED microscope (Leica Microsystems Pty Ltd., USA). The USB2000+ miniature fiber optic spectrometer (Ocean Optics Inc., USA) was coupled to a multimode fiber with the collecting facet mounted in the conjugate image plane of the microscope, via the trinoccular camera port. The microscope was equipped with an N PLAN L 40×/0.55 air objective, an epi-illumination brightfield slider and a ProgRes CFscan camera (JENOPTIK Laser, Optik, Systeme GmbH, Germany) for capturing the reflectance images of particles. The collecting aperture of the fiber-coupled spectrometer had a diameter of 100 $\mu$m which correponded to an effective collecting spot of approximately 3 $\mu$m at the sample plane. Reflectivity spectra were recorded by a LabVIEW script and processed using Origin 8.0 (OriginLab, MA, USA).

Fluorescence images of PSi particles and HeLa cells were obtained with the same Leica DM IL microscope, fitted with a mercury short-arc reflector lamp. The green fluorescence from GFP was detected with an excitation filter: BP470/40, a dichroic mirror: 500 and an emission filter: 525/50. Red fluorescence from the mCherry protein was detected with an excitation filter: BP545/50, a dichroic mirror: 565 and an emission filter: 610/75. The images were recorded with the ProgRes Capture Pro 2.7 software (JENOPTIK Laser, Optik, Systeme GmbH, Germany) and processed with ImageJ 1.42q. Statistic analysis such as one-way ANOVA was performed with GraphPad Prism 5.0.

Scanning electron microscopy (SEM) images of PSi particles were taken using a Hitachi S900 SEM with a cold field emission source (4 kV). The particles were mounted on a brass sample base using carbon tape.

## ■ ASSOCIATED CONTENT

### Ⓢ Supporting Information

Supplementary figures and text outlining SEMs and optical properties of porous silicon particles and evidence of functionality of antibodies bound to the porous silicon particles. This material is available free of charge via the Internet at http://pubs.acs.org.

## ■ AUTHOR INFORMATION

### Corresponding Author

*E-mail: Justin.gooding@unsw.edu.au.

### Notes

The authors declare no competing financial interest.

## ■ ACKNOWLEDGMENTS

The authors wish to acknowledge the generous financial support from the Australian Research Council (DP110102183), Australian Research Council Centre of Excellence in Convergent Bio-Nano Science and Technology (project number

CE140100036), and the National Health and Medical Research Council (project grant APP1024723).

## REFERENCES

(1) Langer, R. (1990) New methods of drug delivery. *Science 249*, 1527−33.
(2) Farokhzad, O. C., and Langer, R. (2009) Impact of nanotechnology on drug delivery. *ACS Nano 3*, 16−20.
(3) Shi, J., Votruba, A. R., Farokhzad, O. C., and Langer, R. (2010) Nanotechnology in drug delivery and tissue engineering: from discovery to applications. *Nano Lett. 10*, 3223−30.
(4) Zhao, W., Schafer, S., Choi, J., Yamanaka, Y. J., Lombardi, M. L., Bose, S., Carlson, A. L., Phillips, J. A., Teo, W., Droujinine, I. A., Cui, C. H., Jain, R. K., Lammerding, J., Love, J. C., Lin, C. P., Sarkar, D., Karnik, R., and Karp, J. M. (2011) Cell-surface sensors for real-time probing of cellular environments. *Nat. Nanotechnol. 6*, 524−31.
(5) Teruel, M. N., and Meyer, T. (2002) Parallel single-cell monitoring of receptor-triggered membrane translocation of a calcium-sensing protein module. *Science 295*, 1910−12.
(6) Sarparanta, M., Bimbo, L. M., Rytkönen, J., Mäkilä, E., Laaksonen, T. J., Laaksonen, P., Nyman, M., Salonen, J., Linder, M. B., Hirvonen, J., Santos, H. A., and Airaksinen, A. J. (2012) Intravenous delivery of hydrophobin-functionalized porous silicon nanoparticles: stability, plasma protein adsorption and biodistribution. *Mol. Pharmaceutics 9*, 654−63.
(7) Foraker, A. B., Walczak, R. J., Cohen, M. H., Boiarski, T. A., Grove, C. F., and Swaan, P. W. (2003) Microfabricated porous silicon particles enhance paracellular delivery of insulin across intestinal Caco-2 cell monolayers. *Pharm. Res. 20*, 110−6.
(8) Mann, A. P., Tanaka, T., Somasunderam, A., Liu, X., Gorenstein, D. G., and Ferrari, M. (2011) E-Selectin-targeted porous silicon particle for nanoparticle delivery to the bone marrow. *Adv. Mater. 23*, H278−82.
(9) Fan, D., De Rosa, E., Murphy, M. B., Peng, Y., Smid, C. A., Chiappini, C., Liu, X., Simmons, P., Weiner, B. K., Ferrari, M., and Tasciotti, E. (2012) Mesoporous silicon-PLGA composite microspheres for the double controlled release of biomolecules for orthopedic tissue engineering. *Adv. Funct. Mater. 22*, 282−93.
(10) Jane, A., Dronov, R., Hodges, A., and Voelcker, N. H. (2009) Porous silicon biosensors on the advance. *Trends Biotechnol. 27*, 230−9.
(11) Gupta, B., Zhu, Y., Guan, B., Reece, P. J., and Gooding, J. J. (2013) Functionalised porous silicon as a biosensor: emphasis on monitoring cells in vivo and in vitro. *Analyst 138*, 3593−615.
(12) Theiss, W. (1997) Optical properties of porous silicon. *Surf. Sci. Rep. 29*, 91−192.
(13) De Stefano, L., Rotiroti, L., Rea, I., Moretti, L., Francia, G. D., Massera, E., Lamberti, A., Arcari, P., Sanges, C., and Rendina, I. (2006) Porous silicon-based optical biochips. *J. Opt. A: Pure Appl. Opt. 8*, S540−4.
(14) De Stefano, L., Moretti, L., Lamberti, A., Longo, O., Rocchia, M., Rossi, A. M., Arcari, P., and Rendina, I. (2004) Optical sensors for vapors, liquids, and biological molecules based on porous silicon technology. *IEEE Trans. Nanotechnol. 3*, 49−54.
(15) Buriak, J. M. (2006) High surface area silicon materials: fundamentals and new technology. *Philos. Trans. R. Soc. London, Ser. A 364*, 217−225.
(16) Foell, H., Christophersen, M., Carstensen, J., and Hasse, G. (2002) Formation and application of porous silicon. *Mater. Sci. Eng., R R39*, 93−141.
(17) Tinsley-Bown, A., Canham, L., Hollings, M., Anderson, M., Reeves, C., Cox, T., Nicklin, S., Squirrell, D., Perkins, E., and Hutchinson, A. (2000) Tuning the pore size and surface chemistry of porous silicon for immunoassays. *Phys. Status Solidi A 182*, 547−53.
(18) Jaganathan, H., and Godin, B. (2012) Biocompatibility assessment of Si-based nano- and micro-particles. *Adv. Drug Delivery Rev. 64*, 1800−19.
(19) Santos, H. A., Riikonen, J., Heikkilä, T., Salonen, J., Peltonen, L., Mäkilä, E., Laaksonen, T., Kumar, N., Murzin, D., Lehto, V. P., and Hirvonen, J. (2008) Biocompatibility of mesoporous silicon microparticles. *Eur. J. Pharm. Sci. 34*, S36−7.
(20) Low, S. P., Voelcker, N. H., Canham, L. T., and Williams, K. A. (2009) The biocompatibility of porous silicon in tissues of the eye. *Biomaterials 30*, 2873−80.
(21) Bimbo, L. M., Sarparanta, M., Santos, H. l. A., Airaksinen, A. J., Mäkilä, E., Laaksonen, T., Peltonen, L., Lehto, V.-P., Hirvonen, J., and Salonen, J. (2010) Biocompatibility of thermally hydrocarbonized porous silicon nanoparticles and their biodistribution in rats. *ACS Nano 4*, 3023−32.
(22) Alvarez, S., Derfus, A., Schwartz, M., Bhatia, S., and Sailor, M. (2009) The compatibility of hepatocytes with chemically modified porous silicon with reference to in vitro biosensors. *Biomaterials 30*, 26−34.
(23) Chiappini, C., Liu, X., Fakhoury, J. R., and Ferrari, M. (2010) Biodegradable porous silicon barcode nanowires with defined geometry. *Adv. Funct. Mater. 20*, 2231−9.
(24) Hon, N. K., Shaposhnik, Z., Diebold, E. D., Tamanoi, F., and Jalali, B. (2012) Tailoring the biodegradability of porous silicon nanoparticles. *J. Biomed. Mater. Res., Part A 100A*, 3416−21.
(25) Park, J.-H., Gu, L., von Maltzahn, G., Ruoslahti, E., Bhatia, S. N., and Sailor, M. J. (2009) Biodegradable luminescent porous silicon nanoparticles for in vivo applications. *Nat. Mater. 8*, 331−6.
(26) Sun, W., Puzas, J., Sheu, T., and Fauchet, P. (2007) Porous silicon as a cell interface for bone tissue engineering. *Phys. Status Solidi A 204*, 1429−33.
(27) Chiappini, C., Tasciotti, E., Serda, R. E., Brousseau, L., Liu, X., and Ferrari, M. (2011) Mesoporous silicon particles as intravascular drug delivery vectors: fabrication, in-vitro, and in-vivo assessments. *Phys. Status Solidi C 8*, 1826−32.
(28) Tasciotti, E., Liu, X., Bhavane, R., Plant, K., Leonard, A. D., Price, B. K., Cheng, M. M.-C., Decuzzi, P., Tour, J. M., Robertson, F., and Ferrari, M. (2008) Mesoporous silicon particles as a multistage delivery system for imaging and therapeutic applications. *Nat. Nanotechnol. 3*, 151−7.
(29) Buriak, J. M., Stewart, M. P., and Allen, M. J. (1999) Functionalization of porous silicon surfaces through hydrosilylation reactions. *Mater. Res. Soc. Symp. Proc. 536*, 173−8.
(30) Kilian, K., Böcking, T., and Gooding, J. (2009) The importance of surface chemistry in mesoporous materials: lessons from porous silicon biosensors. *Chem. Commun.*, 630−40.
(31) Cai, W., Peck, J. R., van der Weide, D. W., and Hamers, R. J. (2004) Direct electrical detection of hybridization at DNA-modified silicon surfaces. *Biosens. Bioelectron. 19*, 1013−9.
(32) Rossi, A. M., Wang, L., Reipa, V., and Murphy, T. E. (2007) Porous silicon biosensor for detection of viruses. *Biosens. Bioelectron. 23*, 741−5.
(33) Wei, S., Wang, J., Guo, D.-J., Chen, Y.-Q., and Xiao, S.-J. (2006) Grafting organic and biomolecules on H-terminated porous silicon from a diazirine. *Chem. Lett. 35*, 1172−3.
(34) Lin, Z., Strother, T., Cai, W., Cao, X., Smith, L. M., and Hamers, R. J. (2002) DNA attachment and hybridization at the silicon (100) surface. *Langmuir 18*, 788−796.
(35) Secret, E., Smith, K., Dubljevic, V., Moore, E., Macardle, P., Delalat, B., Rogers, M.-L., Johns, T. G., Durand, J.-O., Cunin, F., and Voelcker, N. H. (2013) Drug delivery: antibody-functionalized porous silicon nanoparticles for vectorization of hydrophobic drugs. *Adv. Healthcare Mater. 2*, 718−27.
(36) Tanaka, T., Mangala, L. S., Vivas-Mejia, P. E., Nieves-Alicea, R., Mann, A. P., Mora, E., Han, H.-D., Shahzad, M. M. K., Liu, X., Bhavane, R., Gu, J., Fakhoury, J. R., Chiappini, C., Lu, C., Matsuo, K., Godin, B., Stone, R. L., Nick, A. M., Lopez-Berestein, G., Sood, A. K., and Ferrari, M. (2010) Sustained small interfering RNA delivery by mesoporous silicon particles. *Cancer Res. 70*, 3687−96.
(37) Kilpeläinen, M., Riikonen, J., Vlasova, M. A., Huotari, A., Lehto, V. P., Salonen, J., Herzig, K. H., and Järvinen, K. (2009) In vivo delivery of a peptide, ghrelin antagonist, with mesoporous silicon microparticles. *J. Controlled Release 137*, 166−70.

(38) Kilpeläinen, M., Mönkäre, J., Vlasova, M. A., Riikonen, J., Lehto, V.-P., Salonen, J., Järvinen, K., and Herzig, K.-H. (2011) Nanostructured porous silicon microparticles enable sustained peptide (Melanotan II) delivery. *Eur. J. Pharm. Biopharm. 77*, 20−5.
(39) Verma, A., and Stellacci, F. (2010) Effect of surface properties on nanoparticle−cell interactions. *Small 6*, 12−21.
(40) Vo-Dinh, T., Alarie, J., Johnson, R., Sepaniak, M., and Santella, R. (1991) Evaluation of the fiber-optic antibody-based fluoroimmunosensor for DNA adducts in human placenta samples. *Clin. Chem. 37*, 532−5.
(41) Tedeschi, L., Domenici, C., Ahluwalia, A., Baldini, F., and Mencaglia, A. (2003) Antibody immobilisation on fibre optic TIRF sensors. *Biosens. Bioelectron. 19*, 85−93.
(42) Ehrhart, J.-C., Bennetau, B., Renaud, L., Madrange, J.-P., Thomas, L., Morisot, J., Brosseau, A., Allano, S., Tauc, P., and Tran, P.-L. (2008) A new immunosensor for breast cancer cell detection using antibody-coated long alkylsilane self-assembled monolayers in a parallel plate flow chamber. *Biosens. Bioelectron. 24*, 467−74.
(43) Conroy, P. J., Hearty, S., Leonard, P., and O'Kennedy, R. J. (2009) Antibody production, design and use for biosensor-based applications. *Semin. Cell Dev. Biol. 20*, 10−26.
(44) Massad-Ivanir, N., Shtenberg, G., Tzur, A., Krepker, M. A., and Segal, E. (2011) Engineering nanostructured porous $SiO_2$ surfaces for bacteria detection via "direct cell capture". *Anal. Chem. 83*, 3282−9.
(45) Bonanno, L. M., and DeLouise, L. A. (2007) Whole blood optical biosensor. *Biosens. Bioelectron. 23*, 444−8.
(46) Bonanno, L. M., Kwong, T. C., and DeLouise, L. A. (2010) Label-free porous silicon immunosensor for broad detection of opiates in a blind clinical study and results comparison to commercial analytical chemistry techniques. *Anal. Chem. 82*, 9711−8.
(47) Guan, B., Magenau, A., Kilian, K. A., Ciampi, S., Gaus, K., Reece, P. J., and Gooding, J. J. (2011) Mesoporous silicon photonic crystal microparticles: towards single-cell optical biosensors. *Faraday Discuss. 149*, 301−17.
(48) Guan, B., Ciampi, S., Le Saux, G., Gaus, K., Reece, P. J., and Gooding, J. J. (2011) Different functionalization of the internal and external surfaces in mesoporous materials for biosensing applications using "click" chemistry. *Langmuir 27*, 328−34.
(49) Borello, E., and Zecchina, A. (1963) Infrared spectra of v-triazoles–I 2-Aryl-v-triazoles. *Spectrochim. Acta 19*, 1703−15.
(50) Borello, E., Zecchina, A., and Guglielminotti, E. (1966) The infrared spectra of 1,2,3-triazole N-oxides. *J. Chem. Soc. (B)*, 1243−5.
(51) Kilian, K. A., Böcking, T., Ilyas, S., Gaus, K., Jessup, W., Gal, M., and Gooding, J. J. (2007) Forming antifouling organic multilayers on porous silicon rugate filters towards in vivo/ex vivo biophotonic devices. *Adv. Funct. Mater. 17*, 2884−2890.
(52) Hollon, T., and Yoshimura, F. K. (1989) Variation in enzymatic transient gene expression assays. *Anal. Biochem. 182*, 411−8.
(53) Stoline, M. R. (1981) The status of multiple comparisons: simultaneous estimation of all pairwise comparisons in one-way ANOVA designs. *Am. Stat. 35*, 134−41.
(54) Santos, H. A., Riikonen, J., Salonen, J., Mäkilä, E., Heikkilä, T., Laaksonen, T., Peltonen, L., Lehto, V.-P., and Hirvonen, J. (2010) In vitro cytotoxicity of porous silicon microparticles: Effect of the particle concentration, surface chemistry and size. *Acta Biomater. 6*, 2721−31.
(55) Qin, Z., Joo, J., Gu, L., and Sailor, M. J. (2013) Size control of porous silicon nanoparticles by electrochemical perforation etching. *Part. Part. Sys. Charact. 31*, 252−6.
(56) Ziauddin, J., and Sabatini, D. M. (2001) Microarrays of cells expressing defined cDNAs. *Nature 411*, 107−10.
(57) Lee, K.-B., Park, S.-J., Mirkin, C. A., Smith, J. C., and Mrksich, M. (2002) Protein nanoarrays generated by dip-pen nanolithography. *Science 295*, 1702−5.
(58) Chen, C. S., Alonso, J. L., Ostuni, E., Whitesides, G. M., and Ingber, D. E. (2003) Cell shape provides global control of focal adhesion assembly. *Biochem. Biophys. Res. Commun. 307*, 355−61.
(59) Cheran, L.-E., Cheung, S., Wang, X., and Thompson, M. (2008) Probing the bioelectrochemistry of living cells. *Electrochim. Acta 53*, 6690−7.